PORT SAID ENGINEERING RESEARCH JOURNAL
Port Said University - Faculty of Engineering
Volume 28 No. 2 pp: 93 : 109

Assessing of Domain Change Sensitivity for Regional Climate Model Simulations (Reg-CM4.3) at Blue Nile Basin

Sherien Zahran [1,*], *Soheir Mansour* [2], *Dina Ibrahim* [3]

[1] *Associate Professor, High Institute for Engineering and Technology El-Obour, K. 21Cairo - Bilbies Road, and Enviromental and Climate Change Research Institute , National Water Research Center ,Egypt, shreena@oi.edu.eg*

2 Associate professor. El-material Faculty of Engineering, Helwan, Cairo, Egypt, mansoursoheir@yahoo.com

3 *Researcher assistant, Environment and Climate Change Research Institute, National Water Research Center, Cairo, Egypt,* Eng-dina2010@hotmail.com

**Corresponding author, DOI: 10.216.8/PSERJ.2024.246497.1277*

Received 11-11-2023
Revised 15-1-2024
Accepted 6-2-2024

ABSTRACT

Climate changes have a great impact on water resource availability and accessibility especially for downstream countries of transboundary rivers. Blue Nile Basin has a major contribution to the Nile basin yield. The fluctuation and changes in climate patterns in terms of precipitation in the Blue Nile Basin affect runoff and then drought and flood management strategies. The regional climate model (RCM) is a good tool for simulating and predicting the change in climate variables for the medium and long term but it has some limitations and uncertainties. Well selection of boundary conditions and parametrization of downscaling techniques for RCM will improve the prediction scenarios with limited uncertainty. This paper examines the sensitivity of changing the boundary conditions of three domains for the regional climate model "REG-CM4.3" at Blue Nile Basin with horizontal resolutions 25 * 25 km ^{2} for all domains. The projections outputs for all domains were investigated during the historical period from 1979 to 2005 using many statistical indicators such as Nash-Sutcliffe efficiency (NSE), Percent bias (PBIAS), cumulative distribution function (CDF), the density function of probability (PDF), the root mean square error (RMSE), observed standard deviation ratio (RSR) ratio, number of wet and rainy spells, and the precipitation concentration index (PCI). The results show that the third Domain configuration will enhance the result of the Reg-CM4.3. The outputs of this study can be used to predict future precipitation and other climate variables till 2100.

Key Words: Blue Nile Basin; climate change; Reg-CM4.3

1 INTRODUCTION

Regional climate models (RCM) are numerical models that simulate the climate of a specific region. The climate of a region is characterized by the large-scale atmospheric circulation and regional forcing such as topography within the region, and how they interact through various physical and dynamical processes [1]. The regional climate models simulate climate features that were not well captured by global climate models (GCMs) because of their course spatial resolution [2]. The nested regional climate modeling from the driving general circulation model (GCM) is a worthwhile approach for regional climate simulations. It uses dynamical downscale which depends on both the lateral boundary conditions that control the large-scale circulation, regional topography, and land cover/land use features being resolved by the model, as well as physics parameterizations that ultimately determine the local changes in the energy, moisture, and momentum as influenced by the large-scale circulation and regional forcing[3]. They solve the equations of the conservation of energy, momentum, and water vapor that govern the atmospheric state. The outputs of RCM should be tested because different factors can cause uncertainties in simulated outputs. These factors include domain size and location, physics parameterization, model resolution, and lateral boundary condition [2]. This issue affect the sensitivity of the simulated regional climate to the domain size and locations of the lateral boundaries and undesirable features as it introduces uncertainties to the simulation results. [4]. Earlier RCM model sensitivity to physics parameterizations and methods of assimilating the lateral boundary conditions have been enhanced by Giorgi et al. [2]. The skill of REGs depends very much on the large-scale data used to drive the model, the model physics, and how the models were configured. Furthermore, the ability of RCMs is measured by how they can reproduce observed climate features to adders the climate change [3]. The RCM model evaluation is achieved primarily by comparing model simulation variables with observations to identified the bias. This is very important process before proceeding to long-term climate simulations and mitigation strategies for the region. In this context, regional climate models (Reg-CM4.3) with different domain scales have been applied to test the more reasonable outputs with the observed climate feature. The Intergovernmental Panel on Climate Change (IPCC) Fourth Assessment Report, and associated materials provide evidence of global climate change, with an emphasis on problems that water resource managers are anticipated to encounter. The IPCC states that there is a chance that climate change will affect several areas where planners of water resources are actively involved. Excessive precipitation and changes in seasonal flow patterns might raise the likelihood of floods and droughts. Future climate scenarios are anticipated to cause them to occur more frequently and/or be more severe [17]. Many researches have been carried out to examine the potential effects for change of climate on the Blue Nile Basin's water supplies [5], [6] ,[7], [8], [9], [10], [14], [15]. Due to the special geography, high population density, diversity of climatic patterns, and low standard of living, the Nile Basin faces significant problems from the effects of climate change. The use of reasonable climate prediction from RCMs and emission scenarios is relevant to the development and management of the water resources in the Nile Basin. Statistical measures are analyzed to assess the variations in the climatic signal for the RCM simulations. [16]. To reproduce actual climate values while resolving systemic errors in climate model simulations, bias correction techniques are applied. [18]. In this research, the sensitivity of the regional climate simulations model to change the domain boundary conditions is tested at Blue Nile Basin. The Blue Nile Basin is one of the most vulnerable regions to the effects of climate change. However, reasonable and right information on potential future changes with high spatial resolution are importance for the development of effective adaptation. So, the goal of this research is to estimate the best projection for the climate model "Reg-CM4.3" using dynamic downscaling techniques with a horizontal resolution of 25*25 km2. Three domains with different boundary conditions will be examined to improve the climate projection outputs and reduce the model uncertainties. The outputs will be used to predict the climatic variables till the year 2100. It may also be utilized with confidence in various adaptation strategies to cope with the impact of climate change in several applications.

2 DATA AND METHODS

Statistical performance indicators were tested for the three domains at different stations representing the watersheds at the Blue Nile Basin. Based on these indicators the best domain will be selected then the model outputs are biased corrected. Furthermore, the climate change in terms of precipitation will be addressed at blue Nile basin seasons which called " Belg, Kireit, Bega".

2.1.Study Area

The Blue Nile River is a significant tributary of the Nile, spanning around 1,450 km, of which 800 km flow in Ethiopia and the remaining portion via

Sudan. Normally, the Blue Nile flows from Lake Tana southward, then westward, through Ethiopia, and north-west into Sudan. Just upstream of Khartoum (Sudan), where it finally meets the White Nile, is the Blue Nile River basin, which has a drainage area of around 310,000 km2. Between latitudes 9°N and 16°N and longitudes 32°E and 40°E, this region includes the majority of Ethiopia and a portion of Sudan. Roughly 62% of the flow that reaches Aswan comes from it [1]. The Blue Nile and its tributaries drain a large portion of Ethiopia's central and southwest highlands, finishing in the lowlands of Sudan. Khartoum is home to the White Nile and Blue Nile waterways. The Blue Nile watershed is distinguished by a notably large fluctuation in elevation, ranging from around 380 m near Khartoum to over 4200 m above sea level (M.S.L.) in the Ethiopian highlands, as may be shown in Figure (1). The summer monsoon, which is mostly concentrated from July to October, provides the majority of the Blue Nile's annual flow more than 80%. This runoff flows directly to Egypt and Sudan, two downstream countries, if Ethiopia is unable to hold it.[2]

The terrain of the Blue Nile, which extends from the Ethiopian highlands to Sudan, has widespread rainfall. The highlands of Sudan get an average of more than 1200 mm of rainfall yearly, but other places receive less than 400 mm. Moreover, their values have evolved dramatically over time [3]. The main mechanisms regulating rainfall over the Blue Nile basin are the East circulation over the Nile and the duration and timing of the seasonal movement of the Inter Tropical Converge Zone (ITCZ).

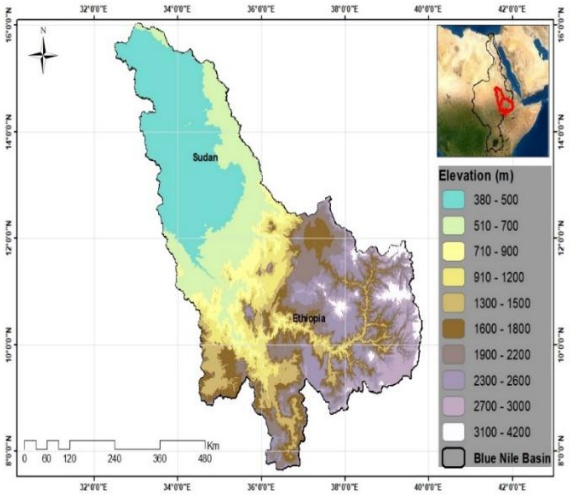

Figure 1: Topography of Blue Nile Basin

The distribution of rainfall in the Blue Nile basin has a unique seasonal pattern all year long. The range in the mean annual rainfall of the Blue Nile subbasin 2000 mm in the Southeast and 110 mm in the North is seen in Figure (2). Out of all the Nile sub-basins, the sub-basin has the greatest average annual precipitation of 1300 mm. The Blue Nile's flow would be mostly impacted by variations in runoff, temperature, rainfall and upstream demand. The climate pattern at Blue Nile Basin is divided into four seasons; in summer, called Kiremt or Meher, which occurs in June, July, and August. It is marked by heavy rainfalls. Spring season, called Belg, occurs in September, October, and November. It is mentioned as the harvest season. Winter season or Bega, occurs in December, January, and February. It is characterized by dry weather with morning frost, especially in January. Autumn, or Tseday, occurs in March, April, and May, and is marked by occasional showers. The warmest month in Ethiopia is May.

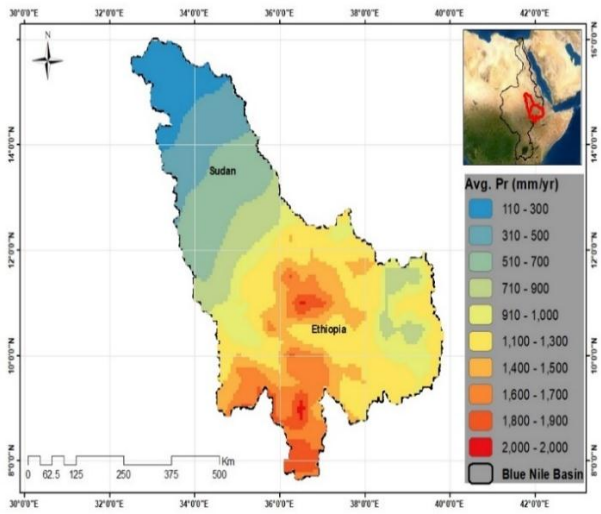

Figure 2: Distribution of average annual rainfall at Blue Nile Basin

2.2. Data Description

In this research the climate model (Reg-CM4.3) is run to simulate the three domains (RCM-1, RCM-2 , RCM-3). Two sources of observed data are tested. The selected one are applied to adjust the model simulation outputs.

2.2.1 Observed Data

Daily data were obtained from 6 meteorological stations in the Basin as in Figure 3, and Table 1 over the period from 1979 to 2005. Historical observed

data was gotten from two sources; first from "Climate Hazards Group InfraRed Precipitation with Station data" (CHIRPS). It is a 35year quasi-global rainfall data set. Spanning 50°S - 50°N (and all longitudes) and ranging from 1981 to near-present, CHIRPS incorporates climatology, CHPclim, 0.05° resolution satellite imagery, and in-situ station data to create gridded rainfall time series for trend analysis and seasonal drought monitoring [6] https://developers.google.com/earth-engine/datasets/tags/precipitation .

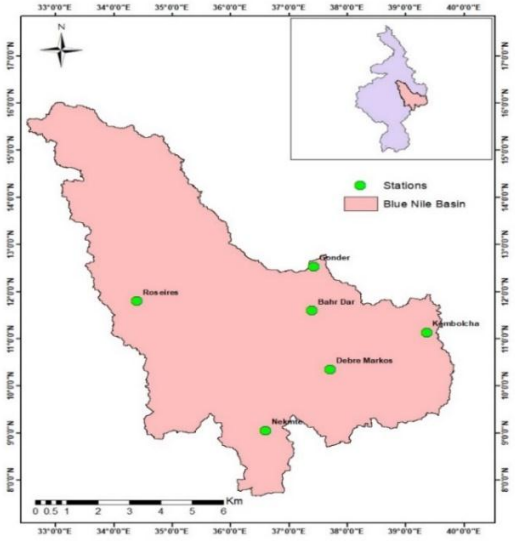

Figure 3: Study Locations at Blue Nile Basin

Table 1. Stations at Blue Nile Basin

Station	Lat.	Lon.
Debre Markos	10.35	37.71
Bahr Dar	11.6	37.4
Roseires	11.8	34.4
Nekmte	9.05	36.6
Gonder	12.53	37.43
Kembolcha	11.08	39.75

Second source from "WFDEI" website for period (1979-2005) . The WFDEI meteorological forcing data set has been generated using the same methodology as the widely used Water and Global Change (WATCH) Forcing Data (WFD) by making use of the ERA-Interim reanalysis data. ERA-Interim is atmospheric reanalysis project which purposes to assimilate historical atmospheric observational data for an extended period. All WFDEI data files have a cell grided center latitude and longitude with 0.5^{o} x 0.5^{o} resolution. Bias correction for precipitation data has been conducted using WFDEI from the Global Precipitation Climatology Centre (GPCC). The GPCC provides monthly precipitation data depend on in-situ observed data from rain gauge networks https://crudata.uea.ac.uk/cru/data/hrg/ . Comparison between two sources of observed data has been done with no significant differences.

2.2.2 Regional climate models

Three simulations of Reg-CM4.3 model ran and examined by dynamically downscaling approach during 1979 to 2005. Each simulation has a special domain boundary condition as shown in figure (4). Table (2) summarizes the Domains configurations system of the Reg-CM4.3 model. The first run (RCM1) examines the area extend from longitude 20^{o}E to 45^{o}E and latitude 0^{o}N to 25^{o}N. The second run (RCM 2) examines a smaller area extend from longitude 30^{o}E to 40^{o}E and latitude 6^{o}N to 16^{o}N. The third run (RCM3) examines Coordinated Regional Climate Downscaling Simulation (CORDEX). It is for all Africa from longitude 25^{o}E to 60^{o}E and latitude 45^{o}N to 42^{o}N. It is under the authorization of "World Climate Research Program" (WCRP). It encompasses many RCMs that could downscale small spatial climate and drive it from a set of (GCMs) within "Coupled Model Inter-comparison Project Phase 5" (CMIP5), 2020 https://cordex.org/. All RCMs simulations have the regraded for grid special resolutions set to 0.22^{0} degree by 0.22^{0} degree for the RCMs. The changes of domains boundaries conditions of dynamic downscaling for the regional climate model (Reg-CM4.3) were examined to define correctly the impact change of climate on this Basin as presented in Figure (4). They were studied and compared for the period from 1979 to 2005. The selected domain based on statistical performance indicators is biased correctly and the future scenarios will be projected. Model outputs include a range of many parameters such; radiation, atmosphere, and surface data. The precipitation will be tested in this research.

Table 2. Domain system configuration for Reg-CM4.3 Simulations

Item	RCM-1	RCM-2	RCM-3 (CORDEX)
Driving Model	MPI-M-MPI-ESM-MR	MPI-M-MPI-ESM-MR	MPI-M-MPI-ESM-MR
Grid number of Points in y direction	100	50	201
Grid number of Points in x direction	100	50	194
No. of Vertical Levels	18	18	18
horizontal resolution in km for Grid point	25	25	25
Model domain "Central latitude in degrees"	12.5 N	11 N	1.31 N
Model domain "Central longitude" in degrees	32.5 E	35 E	17.6 E
Map Projection	Normal Mercator	Normal Mercator	Normal Mercator

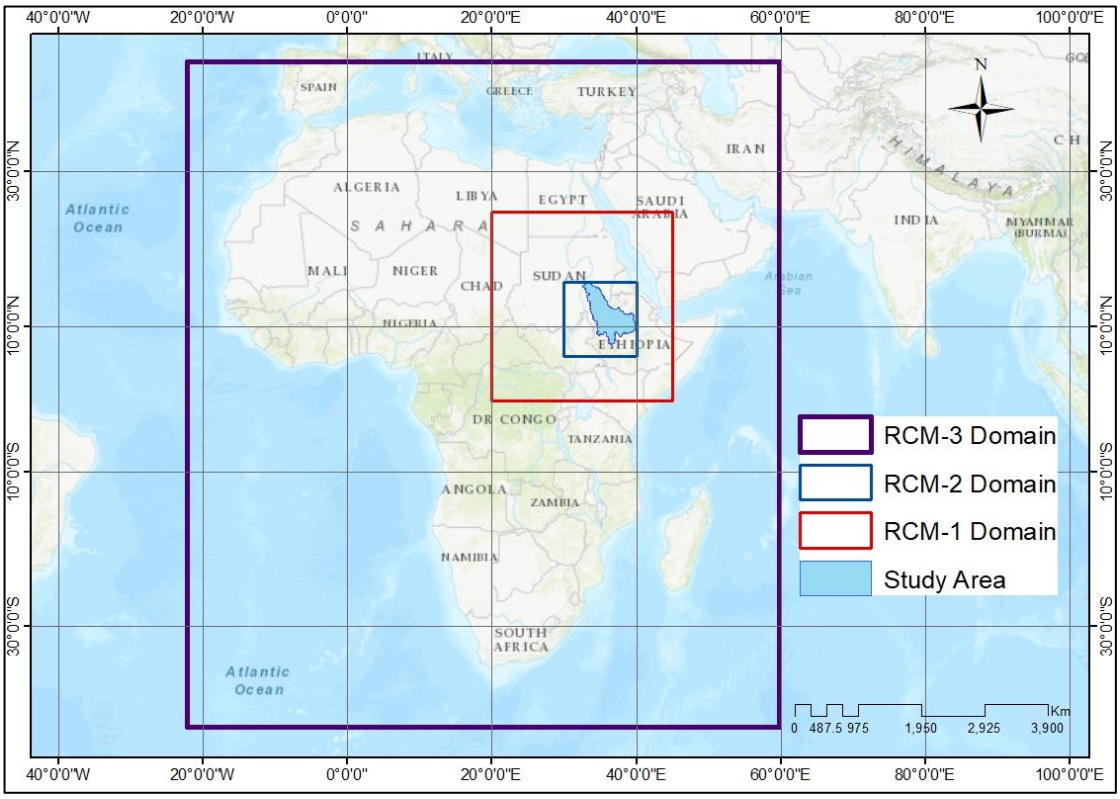

Figure 4: RCMs Domains on the study Area "Blue Nile Basin"

2.3 Data Evaluation Test

A variety of statistical performance metrics are examined in order to assess the quality of the simulation climate models. The data analysis in this study mostly falls under the areas of trend analysis and variability. Nash-Sutcliffe efficiency (NSE), Percent bias (PBIAS), the cumulative distribution function (CDF), the density function of probability (PDF), the root mean square error (RMSE) - observed standard deviation ratio (RSR) ratio, the number of wet and rainy spells, and the precipitation concentration index (PCI) are some of the evaluation techniques.

A) **Percent bias (PBIAS)**

The average tendency of the simulated values to be more or less than their observed ones is measured by percent bias (PBIAS) [9]. PBIAS should ideally be at 0.0, with low magnification values showing precise model simulation. Model underestimation bias is shown by negative values, and overestimation bias is indicated by positive values [10].

The most basic method of bias correction, known as linear scaling (LS), has been utilized in a number of researches [1, 6, 10, 11] to modify the RCM mean value. To produce bias adjusted climate data, the model data is subjected to a difference between the daily observed and model data. The LS approach made use of the following equations:

$$P_{Bias} = \frac{\sum_{i=1}^{n}(P_i^{sim} - P_i^{obs})}{\sum_{i=1}^{n}(P_i^{obs})} * 100 \qquad (1)$$

Where P_{Bias} :is the deviation, given in percentage terms, of the examined data. P_i^{obs} is an observed precipitation data and P_i^{sim} historical simulate raw RCM data.

B) **Precipitation concentration index (PCI)**

The calculation for the concentration of precipitation index (PCI) [5] is as follows:

$$PCI_{annual} = \frac{\sum_{i=1}^{12} Pi^2}{(\sum_{i=1}^{12} Pi)^2} * 100 \qquad (2)$$

where: Pi is the amount of precipitation in month i and the values of PCI are classified as shown in Table (3).

Table 3. Classification of PCI values [7]

PCI Value (%)	Concentration Description
<10	Uniform precipitation distribution (Low Concentration)
11 to 15	Moderate precipitation distribution
16 to 20	Irregular distribution (Concentrated)
>20	Strong irregularity of precipitation distribution

C) **Probability density function (PDF)**

The connection between observations and their probability is known as the probability density. A random variable can have high probability density outcomes as well as low probability density outcomes. Probability distribution refers to the general form of the probability density. A probability density function (PDF), calculates the probabilities for certain possibilities of a random variable. It is useful to know the PDF for a data sample to know whether the observation is unlikely, or so likely as to be considered an anomaly or an outlier that it should be removed. In this research, the PDF for observed data and simulated model simulations are compared to know whether the two have the same behaviors or not. And also test the reasons for the shift of climate variables if there.

D) Nash-Sutcliffe Efficiency (NSE)

The relative amount of the residual variance concerning the variance of the measured data may be determined using a normalized statistic known as the Nash-Sutcliffe efficiency (NSE) [8]. The NSE displays the fit of the simulated data to the 1:1 line with the observed data. NSE is determined in this approach

$$NE1 - \frac{\sum_{i=1}^{n}\left(Y_i^{obs} - Y_i^{model}\right)^2}{\sum_{i=1}^{n}(Y_i^{obs} - Y_i^{mean})^2} \qquad (3)$$

Where Y_i^{obs} is the observed precipitation value and Y_i^{model} is the simulation of precipitation value of the model Y_i^{mean} is the mean of the observed value. A perfect fit between the model and the observed data is indicated by an NSE of 1. When the mean of the observed data is less than the model's predictions, NSE = 0. When the observed mean over-predicts the model better, the value of Inf < NSE < 0. Performance rating for NSE is shown in Table (4),[12].

Performance Rating	NSE
Very good	0.75 ≤ NSE ≤ 1.0
Good	0.65 ≤ NSE ≤ 0.75
Satisfactory	0.5 ≤ NSE ≤ 0.65
Unsatisfactory	NSE < 0.5

Table 4. Performance Rating of NSE

E) RMSE- observations standard deviation ratio (RSR)

One of the often-utilized error index statistics is the routine mean square error (RMSE) [13]. RMSE observations standard deviation ratio (RSR), modified model evaluation measure, was created by [14]. It incorporates both an error index and the standardization of RMSE using the standard deviation of the data. The formula below illustrates how to compute RSR, which is the product of the observed data's standard deviation and RMSE. RSR incorporates a scaling/normalization factor together with the benefits of error index statistics to make the reported values and final statistic adaptable to a variety of components. A large positive number represents an ideal RSR, and a value of 0 indicates a very good model simulation with 0% RMSE or residual variance. The less, the lower the RSR

$$RSR = \frac{RMSE}{STDEV} - \frac{\sqrt{\sum_{i=1}^{n}(Y_i^{obs} - Y_i^{model})^2}}{\sqrt{\sum_{i=1}^{n}(Y_i^{obs} - Y_i^{mean})^2}} \quad (4)$$

Where Y_i^{obs} is the observed value and Y_i^{model} is the simulation value of the model Y_i^{mean} is the mean of observed value.

Table 5. The classification of the Performance Rating of RSR

Performance Rating	**RSR**
Very good	0.0 ≤ RSR ≤ 0.5
Good	0.5 < RSR ≤ 0.6
Satisfactory	0.6 ≤ RSR ≤ 0.7
Unsatisfactory	RSR > 0.7

F) Indicator of wet and dry spell years

For each station, a transformed annual precipitation departure Z may be used to determine the regional distribution of the number of wet and dry years as follows:

$$Z = \frac{x - \mu}{\sigma} \quad (5)$$

where σ is the annual precipitation standard deviation, μ is the annual mean precipitation, and x is the yearly precipitation. When Z < -0.5, there was a dry year; when Z > 0.5, there was a rainy year [4].

2.4 Bais correction

Because of their low geographical resolution, oversimplified physics and thermodynamics, their numerical methods, or their lack of understanding of the workings of the climate system, climate models show systematic inaccuracy (biases). The use of bias correction in climate impact modeling is common. Its primary goal is to modify a subset of a climate model simulation's statistics such that they more closely resemble observable data collected during the current reference period [12]. The linear scaling approach was used in this study's bias correction process, which ran from 1975 to 2005. The monthly adjusted values used in this technique are determined by dividing the raw RCM data by the observed data. It is represented by the following equation.

$$P_{cor,m,d} = p_{,raw,m,d} * \left(\frac{\mu,(P_{obs.,m})}{\mu\ (P_{raw,m})}\right) \quad (6)$$

Where:

$P_{cor,m,d}$ corrected value of precipitation monthly or daily.

$P_{raw,m,d}$ raw value of precipitation monthly or daily.

$P_{obs.,m}$ Observed value of precipitation monthly or daily.

μ symbolizes the operator of expectation (e.g., μ Pobs),

m symbolizes the average amount of precipitation observed during a specific month (m).

3 RESULTS AND DISCUSSION

The results from the Regional Climate Models simulations and the observed date at the six locations are displayed in this part. Watch and CHRIPS data are compared to choose the best performance one. The statistical testes outputs are evaluated for the climate model simulations. Furthermore, the optimum

simulation is applied to reproduce the precipitation projections at the different catchments in the basin.

3.1 Watch and CHRIPS comparison

It is clear from Figure (5) that there is a consistency between Watch and CHRIPS at all stations in the Basin except slightly different at Nekmte and Kembolcha with the same trends during the period of (1979:2005). The Average Historical precipitations for example were highest in June, July, August, and September where the greatest values were in July with a value of 401 mm at Nekmte,352,6 mm at Bahr Dar, and 297.6, 251.5, 192.5 mm at Gonder, Kembolcha, and Roseires respectively. Also, at August was 313.4 mm at Debre Markos.

3.2 Simulations selection

Comparison between the three domain outputs for monthly precipitation at all selected locations are conducting before and after biased correction. Figure (6) shown the average monthly precipitation for the three runs of (Reg-CM4.3); "RCM 1,RCM 2,RCM 3" at the historical period from 1979 to 2005. It is noted that the results of the regional climate model's outputs reflect the same behavior with different values for the study areas. It is clear that the values of REG 1 and RCM 3 are closed at Rosieres, Baher Dar, Goder, and Debra Marcos but the values of RCM 1 and RCM 2 are closed at Nekmte and Kembolocha. Statistical indicators for three Simulations observed before biased corrections during the period of (1975-2005) are presented in Table (6). The precipitation mean values of RCM 1 and RCM 3 are 105.8 and 103.7 respectively which are close to the observed (CRU) (106.3). The same results for the median are shown. The standard deviation (STDV) for RCM 1 and RCM 3 are better than RCM 2. The values of Nut-Sutcliff (NSE) are underestimated for RCM 1 and RCM 3 and overestimated for RCM 2. RCM 1 addressed the least values for P_{bias} and mean absolute error (MAE). From these findings, the RCM 3 could be considered the best run to simulate the future projection of climate parameters after the bias is corrected.

3.3 Performance Indicators

Several performance indicators have been analyzed in this section to determine the optimum run with its boundary condition for future projection at the study area.

3.3.1 Concentration of Precipitation Index (PCI)

The Concentration of Precipitation Index (PCI) is used to evaluate the concentration and variability of precipitation. It is used based on monthly precipitation over 30 years from 1979 to 2005 at the studied locations for observed and simulated data models. The results clarified that according to [15] and referring to table (3), all values of PCI are between 11 to 45 which means it is considered high and very high concentration with some years in the Moderate zone as shown in Figures (6). This could be resulting from differences in boundary conditions of the driving GCMs models 'parametrizations or other sources of data uncertainty that need further sensitivity analysis and correction before use in producing the future projections and then applied in adaptation strategies or other hydrologic applications. Table (7) illustrates the range of variability for the PCI at all stations. The PCI range for RCM 3 is closer than RCM1 and RCM 2 to the observed values for the whole studied period and is classified as moderate to irregular concentration. Hence, the results show that RCM 3 enhanced the result of the model. This could be attributed to the fact that the first run area contains Yamen Mountain, which causes noise in its results. However, the RCM 3 (Cordex data) gets the best results as shown later.

3.3.2 Indicators of Wet And Dry Years

The study locations' spatial distribution of the number of dry ($z < -0.5$) and wet ($z \geq 0.5$) years during 26 years is displayed in Table (8).

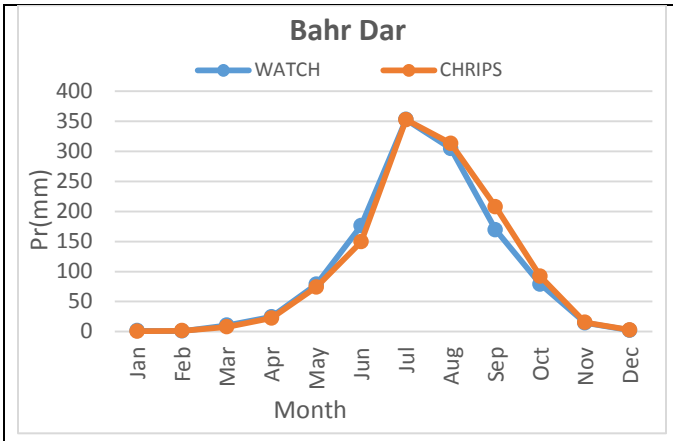
Bahr Dar
WATCH
CHRIPS
Pr(mm)
400
350
300
250
200
150
100
50
0
Jan
Feb
Mar
Apr
May
Jun
Jul
Aug
Sep
Oct
Nov
Dec
Month

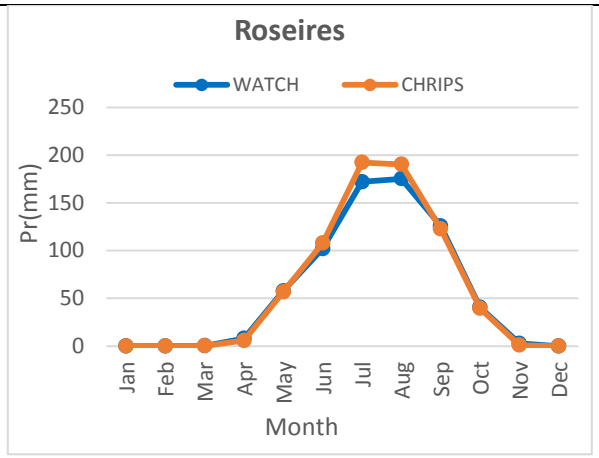
Roseires
WATCH
CHRIPS
Pr(mm)
250
200
150
100
50
0
Jan
Feb
Mar
Apr
May
Jun
Jul
Aug
Sep
Oct
Nov
Dec
Month

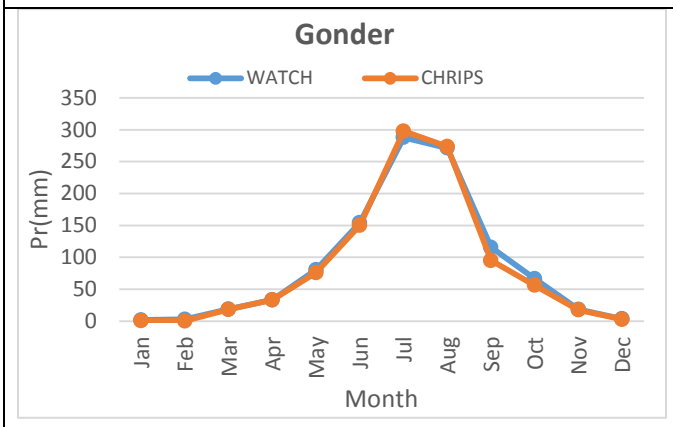
Gonder
WATCH
CHRIPS
Pr(mm)
350
300
250
200
150
100
50
0
Jan
Feb
Mar
Apr
May
Jun
Jul
Aug
Sep
Oct
Nov
Dec
Month

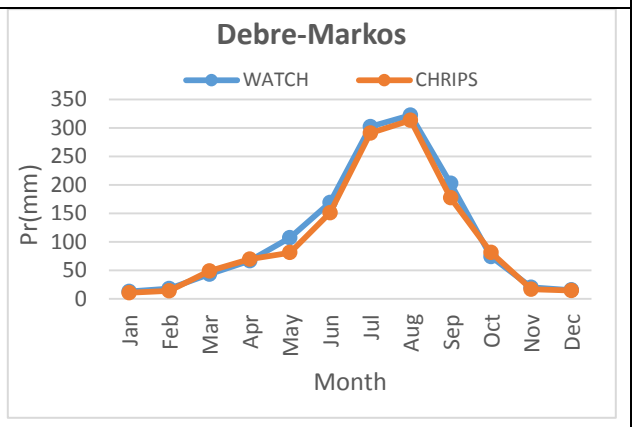
Debre-Markos
WATCH
CHRIPS
Pr(mm)
350
300
250
200
150
100
50
0
Jan
Feb
Mar
Apr
May
Jun
Jul
Aug
Sep
Oct
Nov
Dec
Month

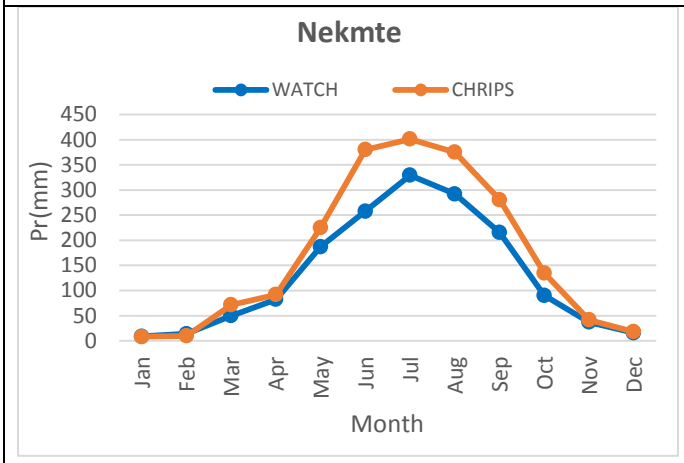
Nekmte
WATCH
CHRIPS
Pr(mm)
450
400
350
300
250
200
150
100
50
0
Jan
Feb
Mar
Apr
May
Jun
Jul
Aug
Sep
Oct
Nov
Dec
Month

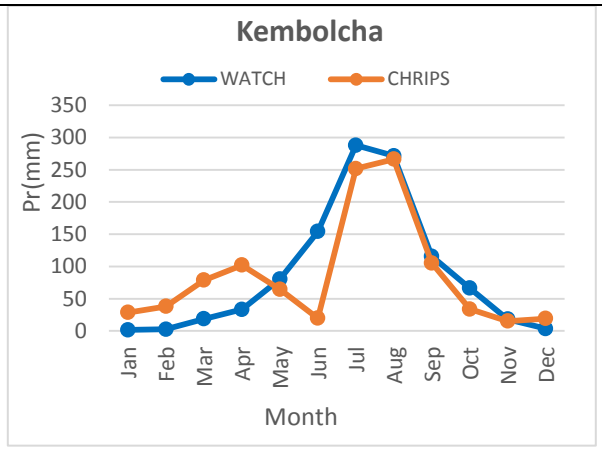
Kembolcha
WATCH
CHRIPS
Pr(mm)
350
300
250
200
150
100
50
0
Jan
Feb
Mar
Apr
May
Jun
Jul
Aug
Sep
Oct
Nov
Dec
Month

Figure 5: Comparison between WATCH and CHRIPS Observed Data during (1979-2005)

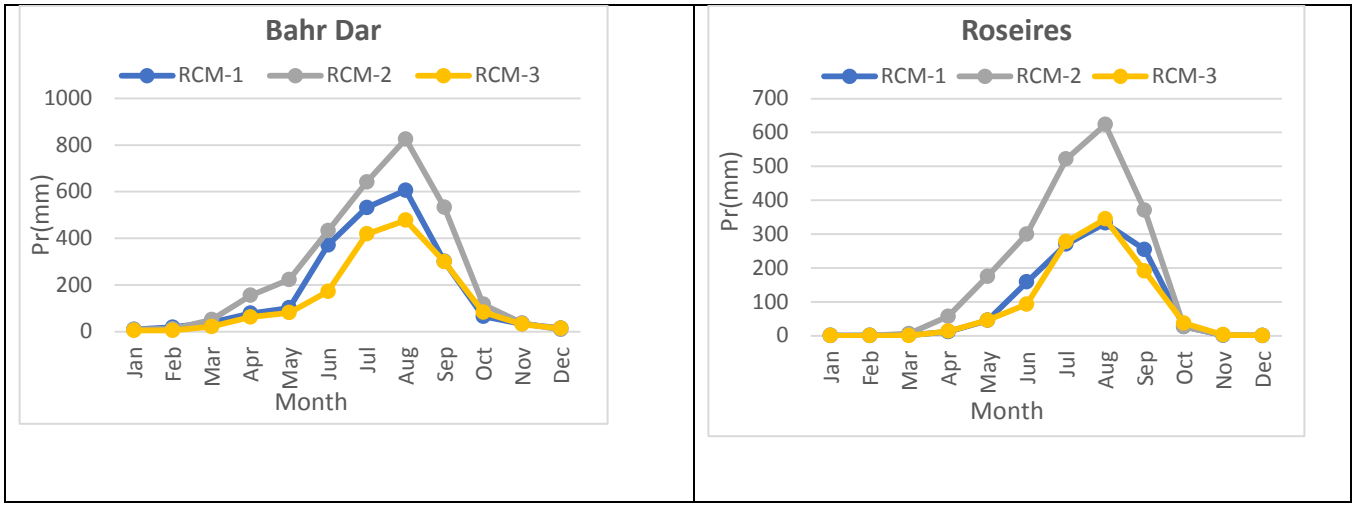

Figure 6: Comparison between three runs Data for Reg-CM4.3 Model during (1979-2005)

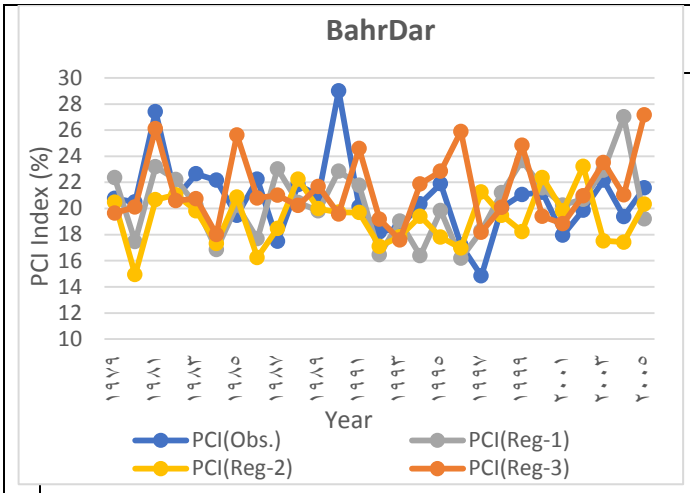
BahrDar
PCI Index (%)
Year
PCI(Obs.)
PCI(Reg-1)
PCI(Reg-2)
PCI(Reg-3)

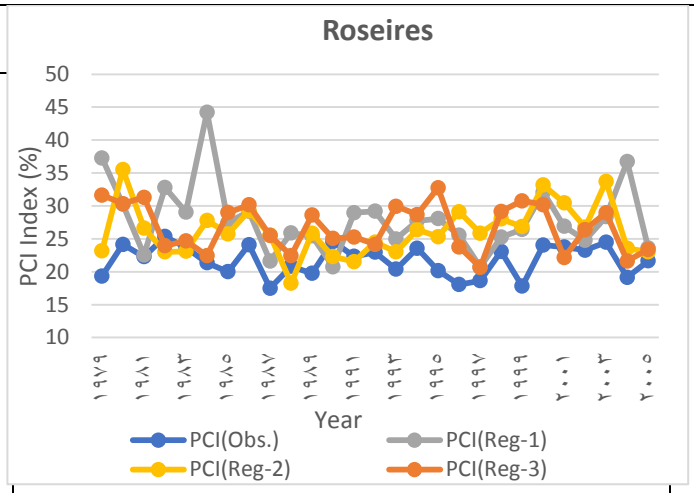
Roseires
PCI Index (%)
Year
PCI(Obs.)
PCI(Reg-1)
PCI(Reg-2)
PCI(Reg-3)

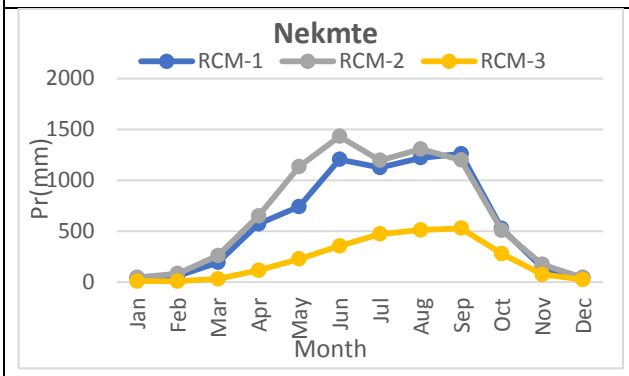
Nekmte
RCM-1
RCM-2
RCM-3
Pr(mm)
Month
Jan
Feb
Mar
Apr
May
Jun
Jul
Aug
Sep
Oct
Nov
Dec

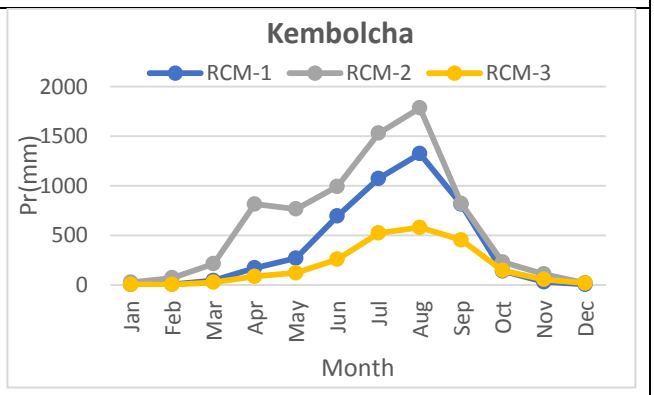
Kembolcha
RCM-1
RCM-2
RCM-3
Pr(mm)
Month
Jan
Feb
Mar
Apr
May
Jun
Jul
Aug
Sep
Oct
Nov
Dec

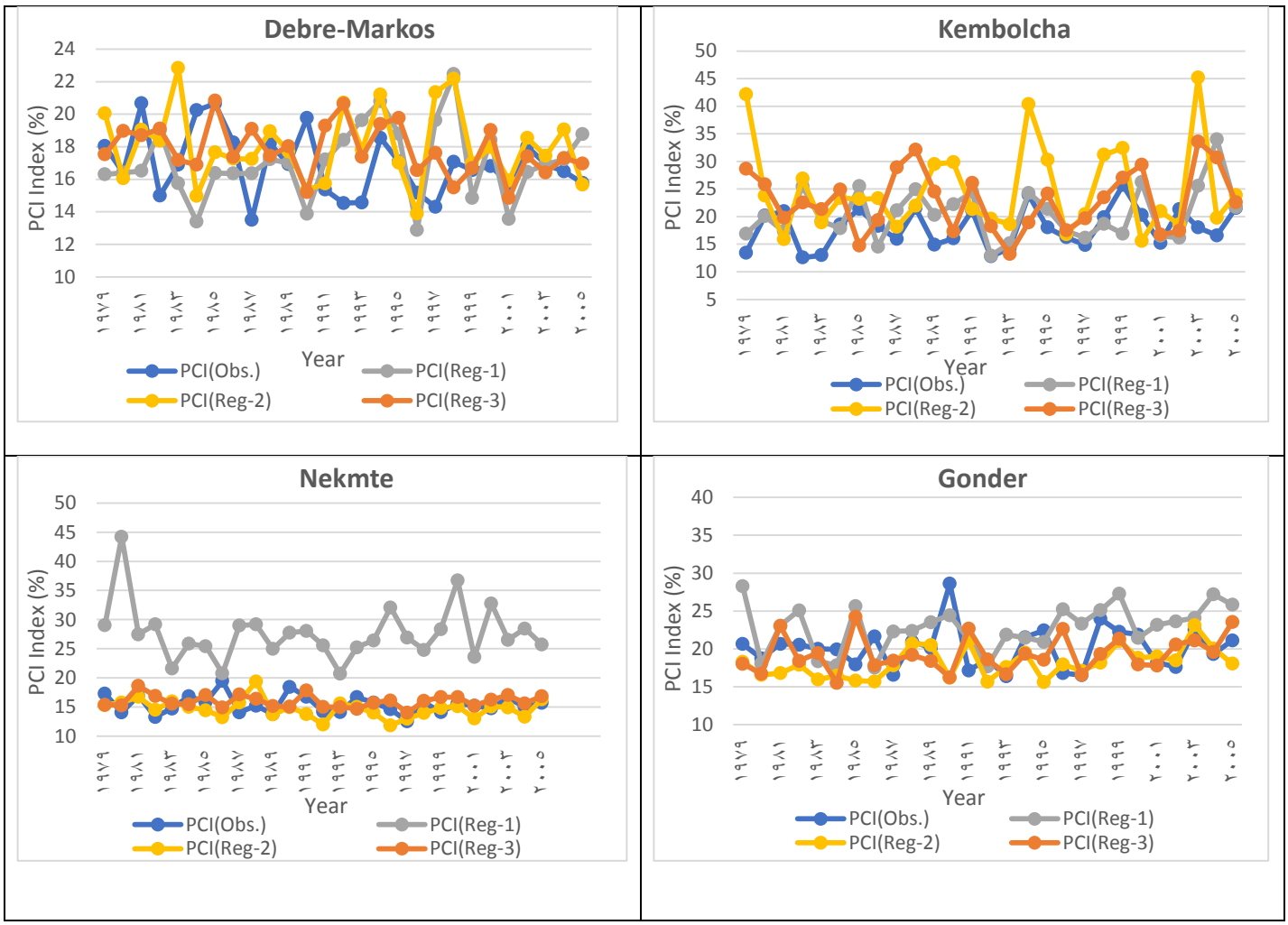

Figure 7: Annual PCI variations during 1979-2005

Table 6. Statistical indicator for three Simulations and observed before biased corrections

Statistics indicators	Simulations			Observed Data
	RCM 1	RCM 2	RCM 3	CRU
Mean	105.79	132.53	103.70	106.33
Median	27.40	42.58	23.36	44.00
STDV	142.2945185	191.4508857	136.0872497	129.1184
NS	-1.74527E-13	5.10703E-15	-3.61933E-14	-

Pbias	0.005069757	-0.197677119	0.025349238	-
MAE	37.40668743	55.40138438	40.94156335	-

Table 7. Precipitation concentration index (PCI) Rang for three simulations and observed during (1975: 2005)

Stations	PCI (min. : max.) Range (%)				Classification
	Simulation Runs				
	Obs.	RCM 1	RCM 2	RCM 3	
Bahr Dar	18:27 (9%)	16 :25 (9%)	16:22 (9%)	18:26 (8%)	Moderate to :irregular
Roseires	18:24 (6%)	21:27 (16%)	21:33 (12%)	22:32 (9%)	Moderate to :irregular
Gonder	16.6:28.6 (12%)	17.8:28.3 (10.5%)	15.6:23 (7.4%)	15.5:24 (8.5%)	Moderate to :irregular
Nekmte	12.8:14.5 (6.7%)	20.8:44.2 (21.4%)	11.9:19.4 (7.50%)	14:17.9 (3.9%)	Moderate to :irregular with strong irregular
Debre-Markos	(13.5:20.6) (7%|)	12.9:22.5 (9.6)	13.9:22.8 (8.9%)	14.8:20.8 (6%)	Moderate to :irregular
Kembolcha	12.6:26.8 (14.2%)	12.9:34 (21%)	15.6:45.2 (29.6%)	13.2:33.6 (20.4%)	Moderate to :irregular with strong irregular

Table 8. Number of wet and dry years for three simulations and Observed data with relative errors during (1975:2005) at Blue Nile Basin

Stations Name	Observed Data		RCM 1		Relative error RCM 1		RCM 2		Relative error RCM 2		RCM 3		relative error RCM 3	
	Dry	Wet	Dry	Wet	dry	wet	Dry	Wet	dry	Wet	Dry	Wet	dry	wet
Bahr Dar	9	7	7	10	22%	33%	13	10	-44%	43%	7	7	22%	0%
Debre-Marcos	12	8	11	7	8%	8%	11	9	8%	13%	10	8	17%	0%
Gonder	8	5	8	7	0%	25%	9	9	-13%	80%	7	5	13%	0%
Kembolcha	5	8	8	7	-60%	20%	10	9	100%	13%	8	9	60%	13%
Nekmte	7	6	10	10	-43%	57%	10	7	-43%	17%	9	6	29%	0%

It provides a true station comparison. In areas like the Blue Nile Basin, where station-to-station distances are great and orography plays a significant role, interpreting the annual rainfall solely based on contour lines is not particularly trustworthy. Based on a review of this table, it can be concluded that the northern mainland and the Lake Tana region have the highest frequency of dry circumstances. The central regions of the mainland region follow suit. Conditions in the southern and western regions are quite damp. Furthermore, by comparing the three simulations with the observed data for the selected stations, it was found that the relative errors at RCM 3 are the smallest values for dry year which are 22%, 17%, 13%, -60%, -29% for Baher Dar , Debre-Marcos, Gonder, Kembolcha, Nekmte, respectively and almost zero for wet years for all stations except Kembolcha , it was 13%. This means that the simulation of RCM 3 is the best run that can represent the future projection for the Blue Nile basin as shown in table (9).

3.4 Bais Correction Results

The Baies correction was applied to enhance the results of the run. The model was tested at the period of

(1975-1990) and (1991-2005) as shown for example in Figures (8) and (9) at Baher Dar. They illustrate that RCM 1 and RCM 3 are better than RCM 2 compared with the observed data for the two periods. Furthermore, as shown in figures (10) and (11) the comparisons using the property density function (PDF) and cumulative density function (CDF) for the three runs during 1975-1990 at Bahr_Dar gave the same results. According to the statistical analysis of mean and standard deviation for all stations during (1979:2005); the monthly precipitation data for the RCM 3 model has a variance around the arithmetic mean at the six locations as shown in Table (9). The greatest value of monthly mean was at Debre-MarKos station with 236 mm then Nekmte with 221.1 mm and the least was at Kembolcha station with 132.9 mm then Roseries and Baher-dar stations with 139.4 and 139.5mm respectively. While Gonder received the mean monthly precipitation of 191.5mm. As illustrated in Table (10) the statistical performance indicators are calculated at all stations after Bais's correction for the regional climate model domain (RCM 3) that gave the best result. The values of Nash-Sutcliffe efficiency (NSE) were found between 0.7 and 0.6 at all stations which are classified between good to very good except at Kembolcha was 0.02, it considered unsatisfactory. Meanwhile, RSR values were 0.38 at Nekmte which is very good, 0.51, and 0.55 at Debre-Markos and Gonder respectively, and are considered good but at Bahr Dar, Roseires, and Kembolcha are satisfactory. Regarding Pbias, Bahr Dar and Kembolcha were overestimated with negligible values tending to zero value and the other stations were overestimated also with very small values. These results indicate that the corrected RCM 3 has a very good performance and could be used for projected future scenarios in the Blue Nile basin. The Bais correction was applied at all runs (RCMs) to correct and enhance the results during 1979:2005. After bias correction, (NSE), (RSR), and (PBIAS) for RCM 3 are calculated and appear good and satisfactory ability to reproduce future projections. Furthermore, during the course of the study period, the PCI range for RCM 3 is more in line with the observed values. The calculation of wet and dry spells annually shows that the RCM 3 has minimum Absolut errors. The analysis of cumulative density function (CDF) and property density function (PDF) for the three runs during 1975-1990 and 1991:2005 gave the same results. Eventually, these results indicate that the corrected RCM 3 has a very good performance and could be used for projecting future scenarios at this basin. we can conclude that as enlarge the buffer zone of boundary conditions, the regional climate model can capture the atmospheric phenomena and avoid the computational troubleshooting errors. Therefore, using this RCM 3 domain will help in the reliable future projections for different climate parameters. Then, drawing the adaptation strategies for climate change that support the decision-makers and increase the resilience of people at the study area could be more realistic.

Table 9. statistical indicators for precipitation data for RCM 3 at the stations during (1979:2005)

Station Name	Mean	Standard Deviation	Standard error	Kurtosis	Skewness
Bahr Dar	139.5	175.6	9.7	0.12	1.23
Roseires	139.4	175.6	9.8	0.12	1.23
Debre-MarKos	236	253	14.1	-0.5	0.88
Gonder	191.5	221	12.3	-0.06	1.09
Kembolcha	132.9	184.9	10.3	3.0	1.9
Nekmte	221.1	212.9	11.8	-1.1	0.58

Table 10. Statistical indicators for RCM 3 after bias corrections

Stations	NSE	RSR	Pbias
Bahr Dar	0.718	0.64	0.025
Gonder	0.729	0.55	-0.13
Roseires	0.718	0.69	-0.13
Nekmte	0.679	0.38	-0.008
Debre-Markos	0.739	0.51	-0.16
Kembolcha	0.02	0.74	0.07

4 CONCLUSIONS

This study examined changes in three domain boundary conditions of dynamic downscaling for the regional climate model to precisely determine the effects of climate change in the Blue Nile Basin (Reg-CM4.3). The region between latitude 0°N and 25° N and longitude 20°E to 45°E is examined in the first simulation (RCM 1). RCM 2 examines a narrower region that spans latitude 6° N to 16° N and longitude 30° E to 40°E. Regional Climate Downscaling Simulation (CORDEX) is the domain that is examined in the third (RCM 3). Throughout 1979–2005, the Bais adjustment was used at every run to improve and rectify the findings. The efficiency of Nash-Sutcliffe (NSE), mean square Root error (RSR), and percentage of bias (PBIAS) for RCM 3 are computed after bias correction, and the results show

that RCM 3 has a good and adequate ability to replicate the future projections. Furthermore, during the span of the study period, the PCI range for RCM 3 is more in line with the observed values. Additionally, the yearly computation of the wet and dry spells demonstrates that the RCM 3 has the least Absolut errors. The same findings were obtained from the examination of the cumulative density function (CDF) and property density function (PDF) for the three runs in 1975–1990 and 1991–2005. The results of this study ultimately show that the adjusted RCM 3 performs extremely well and may be used for the Blue Nile basin's future scenario projections. we can conclude that as enlarge the buffer zone of boundary conditions, the regional climate model can capture the atmospheric phenomena and avoid the computational troubleshooting errors for the same resolutions. Furthermore, accurate future estimates for various climatic parameters will be helpful to use this domain of the regional climate model. subsequently, it might be more realistic to illustrate climate change adaptation strategies that support policymakers and strengthen local populations.

References

[1] Russo, E., Kirchner, I., Pfahl, S., Schaap, M., and Cubasch, U.: Sensitivity studies with the regional climate model COSMO-CLM 5.0 over the CORDEX Central Asia Domain, Geosci. Model Dev., 12, 5229–5249, https://doi.org/10.5194/gmd-12-5229-2019, 2019.

[2] Dadi, D.K., Tesfaye, K., Alemayehu, Y. *et al*. Observed and projected trends of rainfall and temperature in the Central Ethiopia. *Arab J* Geosci 17, 45 (2024). https://doi.org/10.1007/s12517-023-11824- 0

[3] Leung, L.R. (2012). Regional Climate Models . In: Meyers, R.A. (eds) Encyclopedia of Sustainability Science and Technology. Springer, New York, NY.https://doi.org/10.1007/978-1-4419-0851-3_363

[4] Xie P, Yatagai A, Chen M, Hayasaka T, Fukushima Y, Liu C Yang S (2007) A gauge-based analysis of daily precipitation over East Asia. J Hydrometeor 8:607–626

[5] Giorgi F, Bi X (2000) A study of internal variability of a regional climate model. J Geophys Res 105:29503–29521

[6] Oliver, J. E. (1980). Monthly precipitation distribution: a comparative index. The Professional Geographer, 32(3), 300-309.

[7] Funk, C., Peterson, P., Lindfield, M., Pedreros, D., Verdin, J., Shukla, S., ... & Michaelsen, J. (2015). The climate hazards infrared precipitation with stations—a new environmental record for monitoring extremes. *Scientific data*, *2*(1), 1-21.

[8] Gocic, M., Shamshirband, S., Razak, Z., Petković, D., Ch, S., & Trajkovic, S. (2016). Long-term precipitation analysis and estimation of precipitation concentration index using three support vector machine methods. *Advances in Meteorology*, *2016*.

[9] (Nash and Sutcliffe, 1970). Nash, J. E., & Sutcliffe, J. V. (1970). River flow forecasting through conceptual models part I—A discussion of principles. *Journal of hydrology*, *10*(3), 282-290.

[10] Yapo, P. O., Gupta, H. V., & Sorooshian, S. (1996). Automatic calibration of conceptual rainfall-runoff models: sensitivity to calibration data. *Journal of hydrology*, *181*(1-4), 23-48.

[11] Gupta, H. V., Sorooshian, S., & Yapo, P. O. (1999). Status of automatic calibration for hydrologic models: Comparison with multilevel expert calibration. *Journal of Hydrologic Engineering*, *4*(2), 135-143.

[12] Shrestha, M., Acharya, S. C., & Shrestha, P. K. (2017). Bias correction of climate models for hydrological modelling–are simple methods still useful?. *Meteorological Applications*, *24*(3), 531-539.

[13] Maraun, D. Bias Correcting Climate Change Simulations - a Critical Review. Curr Clim Change Rep 2, 211–220 (2016). https://doi.org/10.1007/s40641-016-0050-x

[14] Moriasi, D. N., Arnold, J. G., Van Liew, M. W., Bingner, R. L., Harmel, R. D., & Veith, T. L. (2007). Model evaluation guidelines for systematic quantification of accuracy in watershed simulations. *Transactions of the ASABE*, *50*(3), 885-900.

[15] Vazquez-Amábile, G. G., & Engel, B. A. (2005). Use of SWAT to compute groundwater table depth and streamflow in the Muscatatuck River watershed. *Transactions of the ASAE*, *48*(3), 991-1003.

Singh, J., Knapp, H. V., Arnold, J. G., & Demissie, M. (2005). Hydrological modeling of the Iroquois river watershed using HSPF and SWAT 1. *JAWRA Journal of the American Water Resources Association*, *41*(2), 343-360.

[16] Oliver, J. E. (1980). Monthly precipitation distribution: a comparative index. *The Professional Geographer*, *32*(3), 300-309.

[17] Tefera, Gebrekidan Worku, Yihun Taddele Dile, and Ram Lakhan Ray. 2023. "Evaluating the Impact of Statistical Bias Correction on Climate Change Signal and Extreme Indices in the Jemma Sub-Basin of Blue Nile Basin" *Sustainability* 15, no. 13: 10513. https://doi.org/10.3390/su151310513

[18] IPCC. Climate Change 2021: The Physical Science Basis. Contribution of Working Group I to the Sixth Assessment Report of the Intergovernmental Panel on Climate Change; Masson-Delmotte, V., Zhai, P., Pirani, A., Connors, S.L., Péan, C., Berger, S., Eds.; Cambridge University Press: Cambridge, UK; New York, NY, USA, 2021. [Google Scholar]

[19] Su, T.; Chen, J.; Cannon, A.J.; Xie, P.; Guo, Q. Multi-Site Bias Correction of Climate Model Outputs for Hydro-Meteorological Impact Studies: An Application over a Watershed in China. Hydro. Process. 2020, 34, 2575–2598.

Conflict of interest: the authors have no conflicts of interest

Authors contributions

Author 1; sets the concept of the study, calculates some indicator, writes and reviews the paper,

Author 2: review and writing the paper,

Author 3: analyzed climate models and calculated some indicators.

Declaration of Competing Interest

The authors declare that they have no known competing financial interests or personal relationships that could have appeared to influence the work reported in this paper.

Declaration of Funding:

Funding: This work was not supported by any organization.

List of symbols :

RCM	Reg (Simulation Domain)
RCM 3	CORDEX
CORDEX	Coordinated Regional Climate Downscaling Simulation
WFDEI	meteorological forcing data set has been generated using the same methodology as the widely used Water and Global Change (WATCH) Forcing Data (WFD) by making use of the ERA-Interim reanalysis data from Climate Research Unit (CRU)
CHIRPS	Climate Hazards Group InfraRed Precipitation with Station Data
CMIP5	Coupled Model Inter-comparison Project Phase 5
GPCC	Global Precipitation Climatology Centre

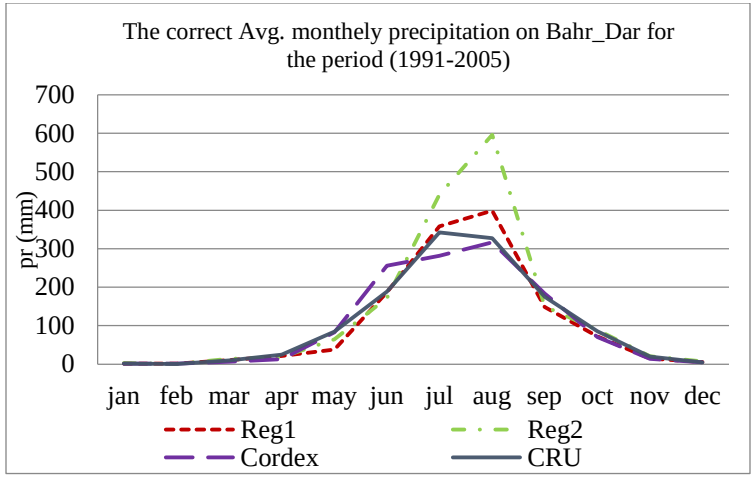

Figure 8: The Correction of Avg. monthly precipitation on Bahr during (1991-2005)

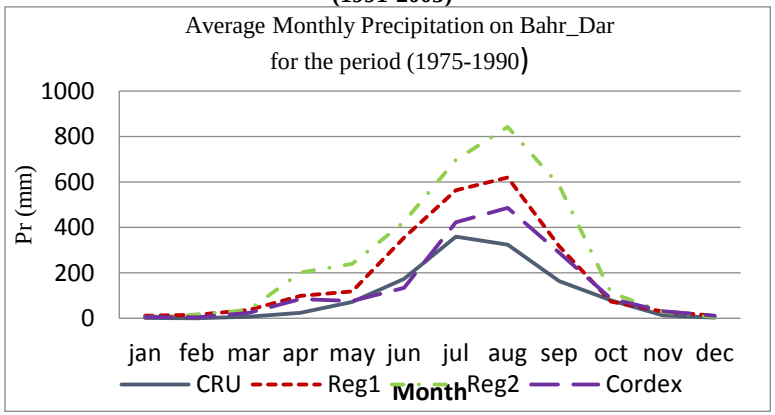

Figure 9: The correction of Avg. monthly precipitation on Bahr_Dar during (1975 -1990))

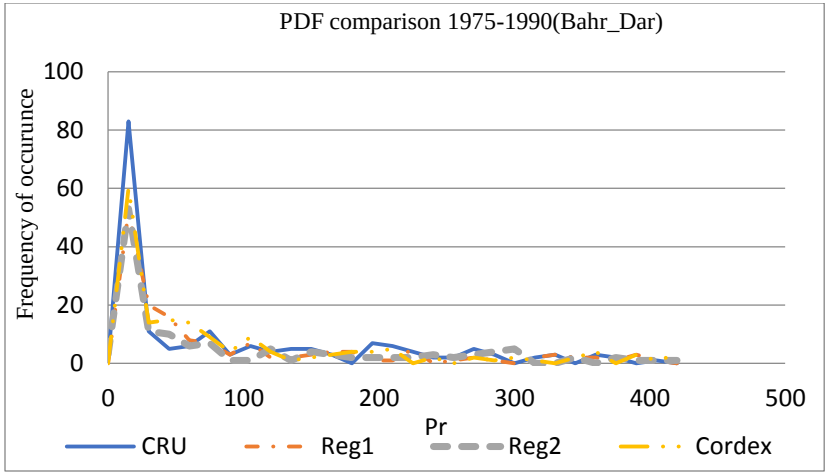

Figure 10: property density function (PDF) comparison for three runs during 1975-1990 at Bahr_Dar

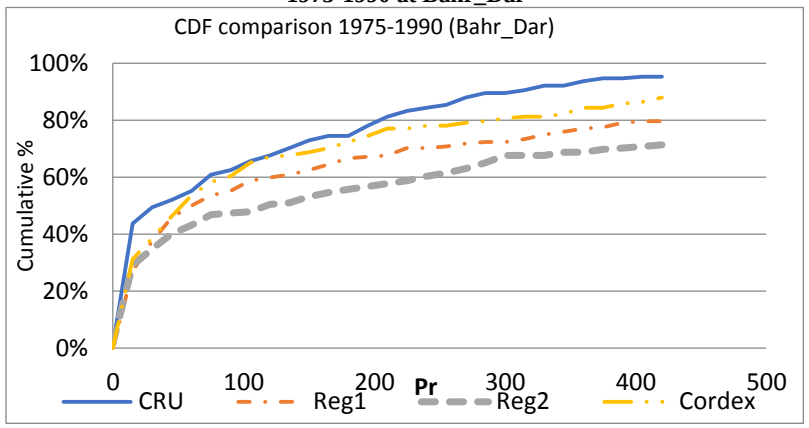

Figure 11: Cumulative density function (CDF) comparison for three runs during 1975-1990 at Bahr Dar